Research Article | Vol. 8, No. 8 | 1 Aug 2018 | OPTICAL MATERIALS EXPRESS 2246
Optical Materials EXPRESS

Nanotrimer enhanced optical fiber tips implemented by electron beam lithography

Ning Wang,[1,*] Matthias Zeisberger,[1] Uwe Hübner,[1] and Markus A. Schmidt[1,2,3]

[1] *Leibniz Institute of Photonic Technology, Albert-Einstein-Str. 9, 07745 Jena, Germany*
[2] *Abbe School of Photonics and Faculty of Physics, Max-Wien-Platz 1, 07743 Jena, Germany*
[3] *Otto Schott Institute of Materials Research, Fraunhoferstr. 6, 07743 Jena, Germany*
[*] *ning.wang@leibniz-ipht.de*

Abstract: Here we present a novel fabrication approach that allows for the implementation of sophisticated planar nanostructures with deep subwavelength dimensions on fiber end faces by electron beam lithography. Specifically, we planarize the end faces of fiber bundles such that they are compatible with planar nanostructuring technology, with the result that fibers can be treated in the same way as typical wafers, opening up the entire field of nanotechnology for fiber optics. To demonstrate our approach, we have implemented densely-packed arrays of gold nanotrimers on the end face of 50 cm long standard single mode fibers, showing asymmetrical resonance lineshapes that arise due to the interplay of diffractive coupling of the individual timer response at infrared wavelengths that overlap with the single mode regime of typical telecommunication fibers. Refractive index sensing experiments suggest sensitivities of about 390 nm/RIU, representing the state-of-the-art for such a device type. Due to its unique capability of making optical fibers compatible with planar nanostructuring technology, we anticipate our approach to be applied in numerous fields including bioanalytics, telecommunications, nonlinear photonics, optical trapping and beam shaping.

OCIS codes: (250.5403) Plasmonics; (060.0060) Fiber optics and optical communications; (310.6628) Subwavelength structures, nanostructures; (110.4235) Nanolithography.

References and links

1. J. A. Schuller, E. S. Barnard, W. Cai, Y. C. Jun, J. S. White, and M. L. Brongersma, "Plasmonics for extreme light concentration and manipulation," Nat. Mater. **9**, 193 (2010).
2. S. A. Maier, *Plasmonics: Fundamentals and Applications* (Springer Science & Business Media, 2007).
3. B. Luk'yanchuk, N. I. Zheludev, S. A. Maier, N. J. Halas, P. Nordlander, H. Giessen, and C. T. Chong, "The fano resonance in plasmonic nanostructures and metamaterials," Nat. Mater. **9**, 707 (2010).
4. F. Aieta, P. Genevet, M. A. Kats, N. Yu, R. Blanchard, Z. Gaburro, and F. Capasso, "Aberration-free ultrathin flat lenses and axicons at telecom wavelengths based on plasmonic metasurfaces," Nano Lett. **12**, 4932–4936 (2012).
5. N. Yu and F. Capasso, "Flat optics with designer metasurfaces," Nat. Mater. **13**, 139 (2014).
6. M. A. Schmidt, D. Y. Lei, L. Wondraczek, V. Nazabal, and S. A. Maier, "Hybrid nanoparticle–microcavity-based plasmonic nanosensors with improved detection resolution and extended remote-sensing ability," Nat. Commun. **3**, 1108 (2012).
7. A. Arbabi, Y. Horie, M. Bagheri, and A. Faraon, "Dielectric metasurfaces for complete control of phase and polarization with subwavelength spatial resolution and high transmission," Nat. Nanotechnol. **10**, 937–943 (2015).
8. A. Tuniz, M. Chemnitz, J. Dellith, S. Weidlich, and M. A. Schmidt, "Hybrid-mode-assisted long-distance excitation of short-range surface plasmons in a nanotip-enhanced step-index fiber," Nano Lett. **17**, 631–637 (2017).
9. N. Bozinovic, Y. Yue, Y. Ren, M. Tur, P. Kristensen, H. Huang, A. E. Willner, and S. Ramachandran, "Terabit-scale orbital angular momentum mode division multiplexing in fibers," Science. **340**, 1545–1548 (2013).
10. B. Doherty, A. Csáki, M. Thiele, M. Zeisberger, A. Schwuchow, J. Kobelke, W. Fritzsche, and M. A. Schmidt, "Nanoparticle functionalised small-core suspended-core fibre–a novel platform for efficient sensing," Biomed. Opt. Express **8**, 790–799 (2017).
11. R. Sollapur, D. Kartashov, M. Zürch, A. Hoffmann, T. Grigorova, G. Sauer, A. Hartung, A. Schwuchow, J. Bierlich, J. Kobelke, M. Chemnitz, M. A. Schmidt, and C. Spielmann, "Resonance-enhanced multi-octave supercontinuum generation in antiresonant hollow-core fibers," Light. Sci. & Appl. **6**, e17124 (2017).
12. G. Kostovski, P. R. Stoddart, and A. Mitchell, "The optical fiber tip: An inherently light-coupled microscopic platform for micro-and nanotechnologies," Adv. Mater. **26**, 3798–3820 (2014).

#332763 https://doi.org/10.1364/OME.8.002246
Journal © 2018 Received 29 May 2018; revised 26 Jun 2018; accepted 1 Jul 2018; published 17 Jul 2018

Optical Materials EXPRESS

13. Y. Lin, J. Guo, and R. G. Lindquist, "Demonstration of an ultra-wideband optical fiber inline polarizer with metal nano-grid on the fiber tip," Opt. Express **17**, 17849–17854 (2009).
14. S. Feng, S. Darmawi, T. Henning, P. J. Klar, and X. Zhang, "A miniaturized sensor consisting of concentric metallic nanorings on the end facet of an optical fiber," Small **8**, 1937–1944 (2012).
15. Y. Lin, Y. Zou, Y. Mo, J. Guo, and R. G. Lindquist, "E-beam patterned gold nanodot arrays on optical fiber tips for localized surface plasmon resonance biochemical sensing," Sensors **10**, 9397–9406 (2010).
16. Y. Lin, Y. Zou, and R. G. Lindquist, "A reflection-based localized surface plasmon resonance fiber-optic probe for biochemical sensing," Biomed. Opt. Express **2**, 478–484 (2011).
17. M. Sanders, Y. Lin, J. Wei, T. Bono, and R. G. Lindquist, "An enhanced lspr fiber-optic nanoprobe for ultrasensitive detection of protein biomarkers," Biosens. Bioelectron. **61**, 95–101 (2014).
18. J. Wei, Z. Zeng, and Y. Lin, "Localized surface plasmon resonance (lspr)-coupled fiber-optic nanoprobe for the detection of protein biomarkers," Biosens. Biodetection: Methods Protoc. Vol. 1: Opt. Detect. pp. 1–14 (2017).
19. C. Liberale, P. Minzioni, F. Bragheri, F. De Angelis, E. Di Fabrizio, and I. Cristiani, "Miniaturized all-fibre probe for three-dimensional optical trapping and manipulation," Nat. Photonics **1**, 723 (2007).
20. H. Sakata and A. Imada, "Lensed plastic optical fiber employing concave end filled with high-index resin," J. Light. Technol. **20**, 638 (2002).
21. D. J. Lipomi, R. V. Martinez, M. A. Kats, S. H. Kang, P. Kim, J. Aizenberg, F. Capasso, and G. M. Whitesides, "Patterning the tips of optical fibers with metallic nanostructures using nanoskiving," Nano Lett. **11**, 632–636 (2010).
22. V. Guieu, P. Garrigue, F. Lagugné-Labarthet, L. Servant, N. Sojic, and D. Talaga, "Remote surface enhanced raman spectroscopy imaging via a nanostructured optical fiber bundle," Opt. Express **17**, 24030–24035 (2009).
23. N. Wang, M. Zeisberger, U. Huebner, and M. A. Schmidt, "Surface lattice resonance assisted hybrid modes in gold trimer arrays," Sci. Reports (submitted) (2018).
24. B. Auguié and W. L. Barnes, "Collective resonances in gold nanoparticle arrays," Phys. Rev. Lett. **101**, 143902 (2008).
25. V. Kravets, F. Schedin, and A. Grigorenko, "Extremely narrow plasmon resonances based on diffraction coupling of localized plasmons in arrays of metallic nanoparticles," Phys. Rev. Lett. **101**, 087403 (2008).
26. S. R. K. Rodriguez, A. Abass, B. Maes, O. T. Janssen, G. Vecchi, and J. G. Rivas, "Coupling bright and dark plasmonic lattice resonances," Phys. Rev. X **1**, 021019 (2011).
27. A. Abass, S. R.-K. Rodriguez, J. Gomez Rivas, and B. Maes, "Tailoring dispersion and eigenfield profiles of plasmonic surface lattice resonances," ACS Photonics **1**, 61–68 (2013).
28. L. Michaeli, S. Keren-Zur, O. Avayu, H. Suchowski, and T. Ellenbogen, "Nonlinear surface lattice resonance in plasmonic nanoparticle arrays," Phys. Rev. Lett. **118**, 243904 (2017).
29. A. W. Snyder and J. Love, *Optical Waveguide Theory* (Springer Science & Business Media, 2012).
30. U. Huebner, M. Falkner, U. D. Zeitner, M. Banasch, K. Dietrich, and E.-B. Kley, "Multi-stencil character projection e-beam lithography: a fast and flexible way for high quality optical metamaterials," in *30th European Mask and Lithography Conference,* (International Society for Optics and Photonics, 2014), p. 92310E.
31. J. Alegret, T. Rindzevicius, T. Pakizeh, Y. Alaverdyan, L. Gunnarsson, and M. Kall, "Plasmonic properties of silver trimers with trigonal symmetry fabricated by electron-beam lithography," The J. Phys. Chem. C **112**, 14313–14317 (2008).

1. Introduction

Understanding the interaction of light with metallic or dielectric nanostructures has revolutionized the field of optics during recent years. By carefully designing the nanostructured elements with respect to material and geometry, effects such as plasmonic nanoconcentration [1], Fano-resonances [2, 3] and beam shaping [4, 5] have been observed, with applications in fields such as enhanced sensing [6], novel optical devices [7, 8], etc.

The key to any of the previously mentioned issues is planar nanostructuring technology, which has experienced substantial advantages during recent times with electron-beam lithography (EBL) representing one of the most applied fabrication approach. However, current EBL nanostructuring technology is mostly limited to planar substrates due to its incompatibility with other types of substrate geometries, having limited the range of potential application of photonic nanostructures which in many situations demand a flexible and remote delivery and collection of the probe light to and from the nanostructures.

Having a functionalized nanostructure at the end of a flexible probe that is compatible with current photonic technology would have enormous impact particular in the field of bioanalytics and medicine. Such a flexible light transportation platform is principally provided by optical fibers. Here the light is confined inside the core of the fiber via total internal reflection and can be

Optical Materials EXPRESS

efficiently guided across very long distances. Due to their unique properties such as light guidance over kilometers length scale, precise control on pulse dispersion and straightforward fabrication optical fibers have revolutionized fields such as telecommunications [9], optical sensing [10] and light generation [11].

Even though optical fibers represent the ideal platform for transporting light to the above-mentioned nanostructures, their small lateral dimensions (typical outer fiber diameter is below 200 μm) and the extremely large aspect ratio are the opposite to what is used in current planar wafer-based fabrication technology, making the combination of planar fabrication approaches and optical fiber technology rather challenging (a detailed review on various fabrication approaches is given in Ref. [12]). Very promising attempts that use EBL to create line gratings [13, 14] and arrays of plasmonic nanodots [15–18] on fiber end faces have been recently conducted. However, the reported most sophisticated geometry - the single dot arrays - shows only a single plasmonic resonance with rather low quality factor (Q-factor) at visible wavelength which is outside the typical operation domain of fiber circuitry (i.e., outside the near infrared (NIR)) and yields only low sensitivity, making it less unattractive for biosensing applications. Other fabrication approaches shown to be useful within the scope of fiber optics include focused-ion-beam milling [19], nanoimprinting [20], nanopattern transferring [21], and chemical etching [22], etc.

In this paper we show the fabrication and characterization of densely packed plasmonic nano-antennas, which are located at the end faces of long optical fibers (approx. 50 cm) and which are realized by electron beam lithography, as it is typically done for planar samples. Specifically, square arrays of gold trimers with precisely engineered deep subwavelength gaps have been successfully patterned on the end faces of step index fibers, showing asymmetrical transmission spectra with strong dips at around 1.65 μm wavelength that result from a coupling of the individual trimer resonance with those of its neighboring unit. The resulting resonance shows a strong red-shift in case the environmental refractive index (RI) is changed, yielding an RI sensitivity of 390 nm/RIU that exceed any of the values reported so far for an EBL-fiber device.

2. The concept of end-face nanostructured optical fibers

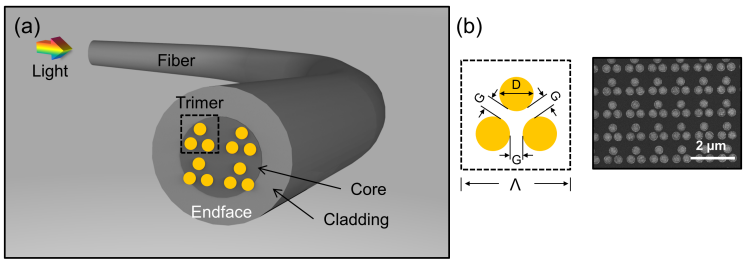

Fig. 1. The concept of nanostructure-enhanced optical fibers. (a) Schematic showing a bent fiber with nanotrimer array at the endface of the fiber (dark grey: core, light gray: cladding). The dashed black square indicates a trimer unit consisting of three identical gold nanodisks. (b) Trimer geometry in square shape unit cell. The left sketch shows the trimer unit including the relevant parameters (D: nanodisk diameter, G: edge-to-edge inter-disk distance). The right scanning electron microscopy (SEM) image shows one example of a fabricated nano trimers array on a fiber end face. In this sample, D and G is around 375 nm and 75 nm respectively with a dot height (i.e., gold film thickness) of 40 nm. The periodical constant (pitch, Λ) is 1.1 μm.

The concept of nanostructured fiber end face (Fig. 1(a)) requires the fabrication of well-defined plasmonic nanoantennas on one facet of an optical fiber. Here we demonstrate this concept by

Optical Materials EXPRESS

combining standard single-mode fibers (Corning SMF-28, single mode cutoff wavelength 1260 nm, mode field diameter 10 μm) with densely packed arrays of gold nanotrimers that is consisted of three identical nanodisks spaced apart by nanometer distances. As shown in a recent work [23] such kind of array exhibits strong resonances at around 1650 nm which lies within the single mode regime of typical telecommunication fibers. The trimers themselves are arranged in a square lattice (inter-trimer unit distance (pitch) 1.1 μm, Fig. 1(b)), with the dot diameter (D), height (H) and interparticle gap (G) given by 375 nm, 40 nm, and 75 nm, respectively. For this densely packed trimer array the resonance wavelength of the trimer unit commensurate with the inter-trimer pitch, leading to the diffractive coupling of the trimer units. Recently reports [24–28] demonstrate that the diffractive couplings (i.e., surface lattice resonances (SLRs))can magnificently alter the optical property (e.g. extinction) of nanopattered surface at almost desired wavelength and generate sophisticated resonance patterns with optical response that greatly exceed the flexible provided by individual nanodot. These unique properties represent our motivation to use arrays of nanotrimer, allows combining a strong nanostructure-mediated resonance with the single mode domain of the fiber used. The SMF-28 reveals a comparably small RI contrast between core and cladding, with the consequence that the propagating mode that reaches the nanostructured can be described in a first-order approximation by a two dimensional Gaussian function [29]. Thus, when the light is coupled into the unstructured side of the fiber, plasmonic resonances are excited by that mode and the overall fiber transmission is modified according to the optical response of the nanostructures.

3. Characterization of optical property of trimer array

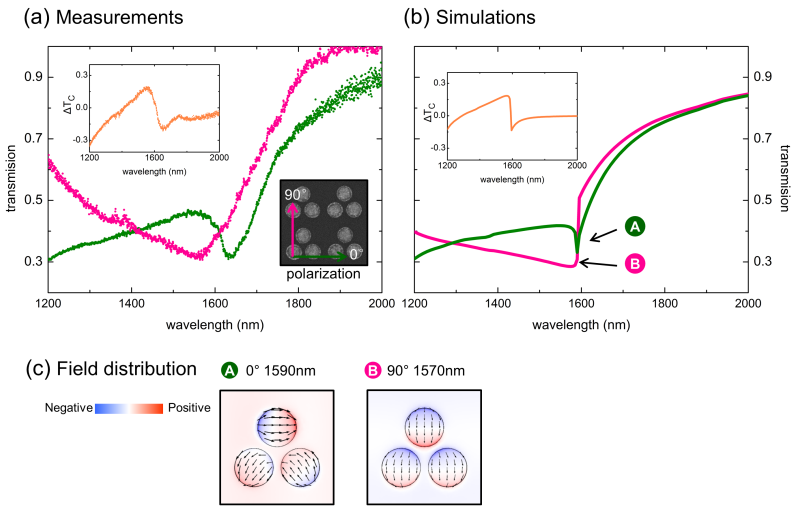

Fig. 2. Spectral distributions of the transmission of nanotrimer arrays located on planar silica substrates ((a) experiment, (b) simulations). The two curves in each plot correspond to the input polarizations along the main symmetry axes of the trimer array (directions defined in the lower inset of (a)). The insets in (a) and (b) show the corresponding transmission contrasts. (c) Simulated near-field patterns of one trimer unit of the array for the configuration labeled by the letters A and B in Fig. 2(b). The color distributions across the disks refer to the z-component (defined in Figure 1) of the electric field 1 nm above the trimer surface, whereas the arrows show the local polarization (i.e., local orientation of the electric at a fixed point of time) in the center plane of dot (height 40 nm)).

As the first step, the optical properties of square arrays of nanotrimers implemented on planar

Optical Materials EXPRESS

substrates are studied. The arrays, fabricated on flat glass by nanopatterning [30], share the same geometry as those created on the fiber end face discussed later (D = 375 nm, H = 40 nm, G = 75 nm, Λ = 1100 nm). The polarization of the probe light (at normal incidence) is set to either 0° or 90°, with the polarization angle being defined as the angle between incident light polarization and the connecting line between the lower two dots (coordinate system in Fig. 2(a), measurement details can be found in Ning et al. [23]). The transmission spectra have been recorded polarization-sensitive using a combination of a broadband light source and suitable diagnostics and are compared to finite-element-method simulations (simulation details are reported in Ref. [23]).

The measured transmission spectra for the two polarization states are shown in Fig. 2(a). A strong transmission dip around 1625 nm is observed for 0° polarization, whereas a weaker and significantly broader dip at around 1575 nm is found when rotating the polarization to 90°. These results clearly show that the transmission of densely-packed trimer arrays is strongly polarization dependent with a lineshape that becomes high asymmetrical especially for 0° polarization, representing behaviors that are not observed sparse trimers arrays [31]. However, for the closely packed trimer array investigated here, the small the inter-trimer distance imposes diffractive couplings of adjacent trimer units particular along the 0°-direction, which further modifies the optical property of the array. Overall the strong polarization dependence of the array is thus a result of the square-shaped lattice breaking the symmetry of trimer geometry, with the small pitch imposing coupling between neighboring trimers. The numerical simulations (Fig. 2(b)) show one transmission dips in either of the two polarization directions (labeled as A and B) in accordance with the experimental observations. The simulated transmission minima are both spectrally located close to the first diffraction order of the glass substrate (n = 1.45). And the simulated electromagnetic field distributions (Fig. 2(c)) reveal that all nanodisks exhibit dipole-like resonance patterns with the local polarization roughly oriented along the direction of the incident light. A more asymmetric distribution is found for two lower trimers for the 0° polarization (point A in Fig. 2(b)), which is a result of the stronger inter-trimer unit coupling due to the smaller spacing between two adjacent trimers for 0°-polarization (275 nm) compared to 325 nm for the 90° situation.

In the following, we would like to introduce the transmission contrast ΔT_c which includes two orthogonally polarized transmission spectra measured under identical experimental configurations. This quantity allows straightforwardly extracting highly polarization sensitive features from the spectral distribution of the transmission measurements and is relevant for the fiber related measurements. In the case of the trimer arrays on a planar surface, the polarization directions are defined with respect to the main axis of the array (angles are defined in the coordinate system in Fig. 2(a)) and the transmission contrast is defined by the following equation:

$$\Delta T_c = \frac{T(0°) - T(90°)}{T(0°) + T(90°)} \tag{1}$$

This quantity is particularly relevant for the analysis of the nanostructure on fiber end faces since the fiber used here (SMF-28) is not polarization maintaining, i.e., the polarization state that reaches the nanostructures is not the same as the input polarization state. We used the following procedure to extract the spectral features of the nanostructures on the fiber end face: First, we measure the spectral distribution of the transmission for various linear input polarization angles. Then we calculate ΔT_c for all combination that is consistent with Eq. (1) and selected the transmission contrast distribution with the strongest fringe depth. The selected situation should then correspond to two linearly and orthogonally polarized input beams across the spectral bandwidth considered. The experimental setup and results can be found in Sec. 5.

The insets in Figs. 2 (a) and 2(b) show the measured and simulated transmission contrasts of the trimer arrays on the planar substrate with all relevant features such as dips and peaks being

Optical Materials EXPRESS

captured. The larger spectral width of the dip results from the fact that the simulations assume plane wave excitation at normal incidence whereas experimentally a Gaussian beam was used that includes a finite range of incidence angles.

4. Fabrication of nanostructures on fiber end faces

The fabrication process to implement nanostructures on fiber end face using EBL is shown in Fig. 3(a) together with corresponding photographs and microscopic images shown in Fig. 3(b). The idea behind our fabrication approach is to planarize the fiber surface such that it is compatible with planar fabrication technology, i.e., that optical fibers can be treated in the same way as typical wafers, opening up the entire field of nanotechnology for fiber optics.

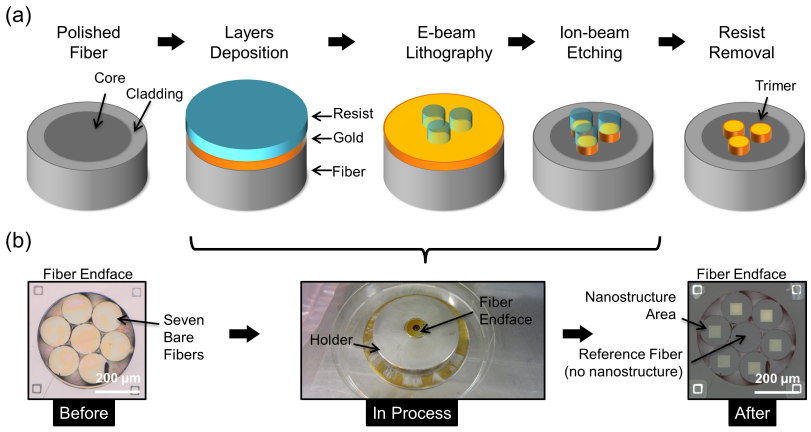

Fig. 3. Electron beam lithography on the planarized sample that contains a bundle of seven standard single mode fibers. (a) Workflow of the nanostructure fabrication process. The planarized fiber end face goes through various steps including nanolayer deposition, e-beam lithography, ion-beam etching and resist removal. (b) Corresponding status of the sample for different fabrication steps.

The details of the fabrication are as follows: A hexagonal bundle of seven SMF-28 fibers is glued into a silica capillary that is then fixed inside a metal holder. This is mechanically polished (Buehler fibermet optical fiber polisher) before spin coating and any lithographic step such that no cracks or corrugations remain visible by eye and microscopic inspection, thus providing a base for spin coating films of resists of precise thickness. This planarized configuration is inserted into a home-made container (diameter: 75 mm, height 12 mm) that is compatible with our EBL machine (Vistec 350OS) and contains the seven fibers with their free ends being winded inside the central holey section of the container. Through vapor deposition and spin coating (micro resist technology GmbH), a 40 nm thick gold film plus a 130 nm thick negative photoresist are coated on the entire holder. It is important to note that the achieved level of planarization is so high that possible thickness variations do not occur in regions that are relevant for the patterning, i.e., only emerge in very close proximity to the edge of each fiber and neither appear across all fibers of the bundle. This in fact yields a reproducibility that is comparable to that of comparable planar nanostructures. By using EBL, the geometry of the nanotrimers arrays are written into the photoresist and ion-beam etching is used to remove the parts of the gold that are not covered by the developed resist. At last, the residues of the resist are chemically removed. To mechanically protect the nanotrimer arrays an alumina film (thickness 10 nm) is deposited on the entire arrangement by atomic layer deposition (plasma enhanced ALD, tool "Oxford Opal"), which has no visible influence on the optical properties of the nano-trimer array as confirmed by

Optical Materials EXPRESS

simulations.

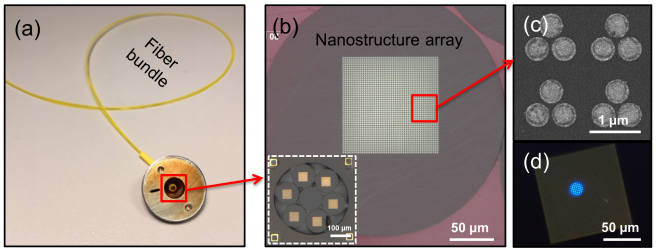

Fig. 4. Images of implemented nanostructures on the fiber end faces and of a fiber bundle. (a) Bundle inside the metal holder that contains six nanostructure-enhanced fibers and an unpatterned fiber (SMF-28). (b) Bright-field microscope image showing one nanotrimer array. The framed image at bottom of (b) shows the overview of fiber bundle after nanostructuring. (c) SEM image of four trimer units on the fiber facet. (d) Image of the output beam spot when white light is coupled into the unstructured part of the fiber. The nanotrimer array consists of 100×100 trimers units and thus overspans the fiber core.

One example of a fiber bundle (fiber length 50 cm) that contains arrays of nanotrimers is shown in Fig. 4(a) with the corresponding SEM images given in Figs. 4(b) and 4(c). Nanostructures are deposited on the outer six fibers of the bundle, whereas the central fiber remains blank and is used as a reference. The width of the array (100×100 trimer units) is chosen such to overspan the core region so that the mode exciting the fiber core fully experiences the impact of the array. The interaction of the mode with the array can be seen straightforwardly when microscopically inspecting the output mode pattern in case white light is launched into the unstructured side of the fiber (Fig. 4(d)) showing a clear and fine-structured spot at the location of the fiber core.

5. Characterization of nanostructures on fiber end faces

As discussed in Sec. 3, the transmission contrast is the key quantity to characterize the performance of the nanostructures on fibers and has been determined here by measuring the spectral distributions of the transmission for various linear input polarizer angles. Light from a supercontinuum white light source (NKT phonics SuperK) is passed through a linear polarizer (Codixx) that was used to control the input polarization and coupled into the unstructured sides of the fibers by a 20 × objective (Olympus). After passing the fiber and the nanotrimer array the output light is guided into an optical spectral analyzer using a multimode fiber (Thorlabs custom fiber). The angle of polarization of the incident light is gradually rotated from 0° to 180° in a step of 10°, whereas the starting polarization angle (0°) was arbitrarily chosen. As a result, 19 transmission spectra and hence 9 transmission contrast distributions are obtained, allowing identifying the polarizer angle under which the spectral features, in particular, the dip at around 1.65 μm having maximal fringe contrasts.The optical power at the input was adjusted such not to exceed 500 μW thus preventing sample damage.

The chosen transmission contrast distribution (yellow) together with the corresponding curves of the planar array (orange) and the reference fiber that contains no nanostructures (green) are shown in Fig. 5(b). A direct comparison of nanoarray-enhanced fiber and planar sample shows a dip at around 1.65 μm for both configurations, clearly revealing the impact of the nanotrimer arrays on the transmission of the fiber. Remarkably, the position of the features of both spectra matches fairly well with the fiber structures showing a greater fringe contrast, emphasizing the quality of the fabricated nanotrimers on the fiber end face. The difference in the shape of the two presented transmission contrast functions we attribute to a non-ideal linear polarization state in the case of the fiber excitation that may result from a coupling between the two LP_{01} modes

Optical Materials EXPRESS

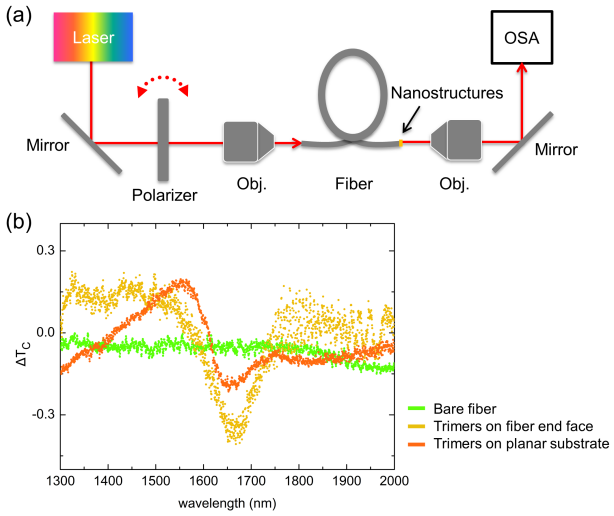

Fig. 5. Transmission contrast measurement setup and obtained results. (a) Experimental setup. The nanostructure-enhanced fiber is bent to eliminate cladding modes (Obj: objective, OSA: optical spectrum analyzer). (b) Spectral distributions of the transmission contrast of nanotrimer arrays on fiber endface (yellow) and planar substrate (orange) with a comparison to a blank fiber (green). The spectral positions of the main dips of fiber and planar samples match well, while the curve of blank fiber (green) shows hardly any features.

supported by the SMF-28. The nanostructure-enhanced fiber shows a unique lineshape that solely arises from the presence of the nanostructures and is not observed for the bare fiber (green curve in Fig 5 (b)), proving that the optical response of optical fibers can strongly be altered by the use of the sophisticated functionalities provided by plasmonic nanostructures.

6. Refractive index sensing

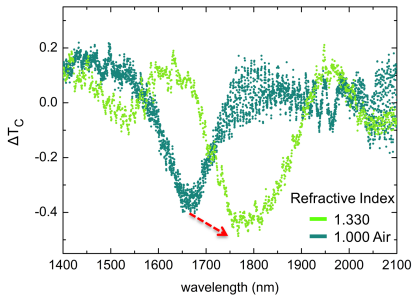

Fig. 6. Spectral distribution of the transmission contrast for a fiber sample having the nanotrimer array exposed to air (dark green) and analyte refractive liquid (light green), with the red arrow indicating the spectral shift of the main dip.

The nanostructure-enhanced fiber principally represents is a promising concept for remote and efficient sensing beyond to what is possible with current fiber probes. To demonstrate its potential, the spectral distribution of the transmission contrast of the nanostructure-enhanced fiber has been additionally measured for the situation the nanostructures are immersed in an aqueous analyte

Optical Materials EXPRESS

liquid (details of the sensing characteristics of the nano-trimer array can be found in Ref. [23]). For these measurements, a glass slide was placed close to the nanostructures (distance between fiber end face and glass slide: about 1 mm) and the gap was filled with analyte refractive liquid (n = 1.33). The measured spectra (Fig. 6) clearly show that the main dip originally located at around 1650 nm (dark green points) shifts to about 1800 nm as the RI increases from 1.0 (air) to 1.33. The resulting RI sensitivity is about 390 nm/RIU which is about two times higher compared to reported LSPR fiber tip sensors (around 190 nm/RIU [15, 16]). Similar RI sensing experiments conducted on identical arrays of nano-trimers implemented on planar glass substrates in the index range from 1.0 to 1.7 (reported in Ref. [23]) show a linear shift of the resonance wavelength at similarly high sensitivity values, confirming the potential of the nano-trimer approach for sensing purposes, particular if being deposited on the end face of optical fibers.

7. Conclusion

Based on massive improvements in fabrication technology, nanostructures have revolutionized photonics within highly relevant fields such as bioanalytics, nonlinear optics, and control of light beams. Particular the creation of planar nanostructures on optical fiber tips principally represents a very promising concept for applications that demand using the unique functionalities and responses of nanostructures on a flexible and efficient waveguide platform. The key challenge here is the intrinsic incompatibility of wafer-based technology with optical fibers since the typical aspect ratio of optical fibers is the opposite to what is used in planar nanofabrication technology.

Here we present a novel fabrication approach that allows implementing sophisticated nanostructures with deep subwavelength dimensions on fiber end faces by electron beam lithography. The overall idea behind our fabrication approach is to planarize the fiber surface such that it is compatible with planar fabrication technology, i.e., that the fibers can be treated in the same way as typical wafers, opening up the entire field of nanotechnology for fiber optics. To demonstrate our approach, we have implemented arrays of nanotrimers on the end faces of standard single mode fibers that have lengths of about 50 cm by integrating bundles of these fibers into a container that allow employing all steps of current nanotechnology. In accordance with simulations and measurements of comparable planar samples, the optical characterization of the nanostructure-enhanced fibers clearly shows the impact of inter-trimer coupling, i.e., the emergence of surface-lattice resonance mediated responses in the transmission spectra. As confirmed by measurements and simulations dense arrays of nanotrimers are particularly attractive for fiber optics since their main optical responses are located within the single mode regime of typical telecommunication fibers (i.e., at around 1.6 μm). Operation in the single mode domain is particular important since only then a precisely defined field pattern without the contribution of higher-order modes at the location of the nano-structures can be ensured. Additionally, we conducted refractive index sensing experiments yielding a sensitivity of about 390 nm/RIU, which is the highest measured value so far reported for a plasmonic fiber end face sensor device.

Due to its unique capability of making optical fibers compatible with planar nanostructuring technology, our fabrication approach is applicable to all types of currently used nanostructures, including metasurfaces, plasmonic nanosensors or nanogratings and is not restricted to metallic structures, i.e., can be straightforwardly extended to dielectrics. Our concept can be applied to almost any kind of e-beam lithographic machine (i.e., the lithographic machine does not need to be modified to fit the fiber geometry) and therefore any type of nanostructure that has been implemented with that infrastructure is accessible. One example demonstrating the advantages of our approach is that it allows to spin coat resists of defined thickness onto the end face of the fibers, which is exceedingly hard if not impossible to achieve in case the fiber end face is not planarized. We anticipate our fabrication approach to be useful for a wide range of applications, including bioanalytics, telecommunications, nonlinear photonics, optical trapping and beam

Optical Materials EXPRESS

shaping. Further modification of the implementation procedure may allow for extending the scheme to fibers made from other materials such as polymers or elastomers.

Funding

Thuringian State (2015FGI0011); European Regional Development Fund; Chinese Scholarship Council (201509110107).

Acknowledgments

This work is partially funded by Thuringian State via the projects 2015FGI0011, and 2015-0021 partially supported by the European Regional Development Fund (ERDF). N. W. acknowledges funding by Chinese Scholarship Council via contract number 201509110107.